



Accepted Article

Title: Plumbagin-Serum Albumin Interaction: Spectral, Electrochemical, Structure-Binding Analysis, Anti-proliferative and Cell Signaling Aspects with Implications for Anticancer Therapy

Authors: Veronique Baron, Adrian Chrastina, John Welsh, gaelle rondeau, parisa abedinpour, and per borgstrom

This manuscript has been accepted after peer review and appears as an Accepted Article online prior to editing, proofing, and formal publication of the final Version of Record (VoR). This work is currently citable by using the Digital Object Identifier (DOI) given below. The VoR will be published online in Early View as soon as possible and may be different to this Accepted Article as a result of editing. Readers should obtain the VoR from the journal website shown below when it is published to ensure accuracy of information. The authors are responsible for the content of this Accepted Article.

To be cited as: *ChemMedChem* 10.1002/cmdc.202000157

Link to VoR: <https://doi.org/10.1002/cmdc.202000157>

Plumbagin-Serum Albumin Interaction: Spectral, Electrochemical, Structure-Binding Analysis, Anti-proliferative and Cell Signaling Aspects with Implications for Anticancer Therapy

Adrian Chrastina^{2§}, John Welsh¹, Gaelle Rondeau¹, Parisa Abedinpour², Per Borgström¹ and Véronique T. Baron^{1§}

¹Vaccine Research Institute of San Diego, San Diego Science Center, San Diego, CA 92109

²Proteogenomics Research Institute for Systems Medicine, La Jolla, CA 92037

§Corresponding authors:

A. Chrastina: current address: Proteogenomics Research Institute for Systems Medicine (PRISM), 505 Coast Blvd. South, La Jolla, CA 92037

V.T. Baron: Vaccine Research Institute of San Diego (VRISD), San Diego Science Center, 3030 Bunker Hill, San Diego, CA 92109, USA. Phone: (858) 775-1736; Email: vbaron@sdibr.org

Running title: Plumbagin-albumin interaction and anticancer activity of plumbagin

Keywords: Prostate cancer, plumbagin, albumin

Disclosures: This work was supported by funds from Pellficure Pharmaceuticals, Inc.

P. Borgström, A. Chrastina, P. Abedinpour and V. Baron are inventors on patent(s) in relation to this work. P. Borgström is President of PellFiCure Pharmaceuticals, Inc. while V. Baron, P. Abedinpour and A. Chrastina are current or former consultants for the company. J. Welsh and G. Rondeau declare no competing interest.

ABSTRACT

Plumbagin (5-hydroxy-2-methyl-1,4-naphthoquinone) is a small molecule with potent anticancer activity. Like other 1,4-naphthoquinones, it exhibits electrophilic reactivity towards biological nucleophiles. We demonstrate that plumbagin and structurally related 1,4-naphthoquinones with at least one unsubstituted quinoid carbon (C2 or C3) bind to albumin, an ubiquitously present nucleophile, with minimum recovery of free drug. Recovery of plumbagin from albumin declined in a one-phase kinetic with a half-life of 9.3min at 10 μ M. Plumbagin in the presence of albumin exhibited instant changes in UV-VIS absorption bands. Electrochemical analysis using cyclic voltammetry showed a decrease in redox peak currents over time until electro-inactivity, suggesting formation of a supramolecular adduct inaccessible to electron transfer. The adduct inhibited cell growth and caused cell cycle arrest of prostate cancer cells, in part by decreasing levels of cell cycle regulator RBBP. The conjugate displayed similar cellular effects as described for plumbagin such as decreased levels of androgen receptor and protein kinase C-epsilon. The effect of plumbagin-albumin on cancer cells was species-specific, suggesting a receptor-mediated mechanism. It was blocked by cathepsin inhibitor pepstatin A, indicating that lysosomal degradation releases plumbagin to the cell. The spontaneous formation of a plumbagin-albumin adduct is likely to have crucial implications for the pharmacodynamics of plumbagin.

INTRODUCTION

Plumbagin (Figure 1A) is a naturally occurring 1,4-naphthoquinone and analog of vitamin K3 isolated from plants of the Plumbaginaceae, Droseraceae, and Ebenaceae families [1, 2]. Purified plumbagin inhibits the proliferation of various types of cancer cells, as reviewed extensively in [3, 4], therefore it is considered a valid oncology drug candidate. *In vivo* studies have shown that it reduces primary tumor burden across cancer types as measured by tumor growth rate as well as tumor weight and volume [4]. Plumbagin inhibits the growth of metastatic foci and delays or suppresses metastatic colonization in mouse models of breast cancer [5], prostate cancer [6] and lung cancer [7]. In addition, the drug appears to improve the efficacy of radiation therapy and of various modalities of chemotherapy in several types of cancer [4]. If these effects are validated, plumbagin may become a useful adjunct to current standard therapy in a variety of settings. In prostate cancer for example, plumbagin was most effective in combination with androgen deprivation therapy, which is the clinical standard of care for hormone-dependent prostate cancer [8, 9]. Plumbagin has now entered clinical trial for the treatment of prostate cancer in combination with androgen deprivation therapy [10].

The pharmacodynamic properties of plumbagin are fundamental for its efficacy in the clinic. Pharmacokinetic analyses indicate that the plasma levels of plumbagin decrease sharply with time in animals, particularly when administered intravenously [11, 12]. The quinoid pharmacophore of plumbagin and other 1,4-naphthoquinones exhibit potent electrophilic reactivity towards biological nucleophiles. The high reactivity of plumbagin added to its rapid plasma clearance suggest that it may rapidly interact with plasma nucleophiles such as serum albumin, which is the most abundant protein in the plasma, contributing to about 60% of the blood proteins (35–50 g/L in human serum). Indeed, structurally related naphthoquinone derivatives bind to bovine serum albumin (BSA) as well as human serum albumin (HSA) *in vitro* [13]. Serum albumin plays a critical role in the maintenance of blood colloidal pressure and acts as a solubilizer and detoxifying protein. It represents the main transport carrier in the blood circulation for fatty acids, ions such as calcium, steroid hormones and many systemically administered pharmaceutical drugs, including antibiotics, anticoagulants, anti-inflammatory drugs, anesthetics, benzodiazepines, etc [14, 15]. Binding of drugs to albumin alters their metabolism, distribution and physiological effects [16, 17]. It increases the solubility of an otherwise poorly soluble drugs and slows its distribution through the tissues while decreasing its side-effects. It also improves the pharmacokinetic profile of the drug since serum albumin has a long half-life of about 19 days owing to its interaction with the Fc receptor [18]. Importantly, serum albumin can potentially

act as an effective carrier for drug delivery to tumors. Several studies in animals showed that albumin is accumulated in tumor tissue due to increased vascular permeability and lack of functional lymphatic system, a mechanism known as enhanced permeability and retention (EPR) [19, 20]. Furthermore, there are several albumin-binding receptors, including gp60 [21], SPARC [14, 22], and scavenger receptors gp18 and gp30 [23] that mediate specific interaction with serum albumin and can facilitate the selective uptake of albumin in tumor tissue.

The present study analyzes the spontaneous interaction of plumbagin with albumin, leading to the formation of a plumbagin-albumin adduct that exhibits anti-proliferative activity against cancer cells. The plumbagin-albumin adduct increased the phosphorylation of AMPK and decreased protein levels of PKC epsilon and AR in prostate cancer cells, which are known effects of plumbagin. The extemporaneous interaction of plumbagin with albumin, a ubiquitously present nucleophile, could have a fundamental influence on the pharmacokinetics and the anticancer activity of plumbagin.

MATERIALS AND METHODS

The 2,3-dimethyl-1,4-naphthoquinone was purchased from SIA MolPort (Latvia, EU). Plumbagin, juglone, naphthazarin, 1,4-naphthoquinone, menadione and other common chemicals were from Sigma-Aldrich (Saint-Louis, MO, USA). Peroxidase-conjugated F(ab')₂ antibodies were from Rockland (Limerick, PA, USA) and the cell cycle sampler kit (611423) was from BD Biosciences (San Jose, CA, USA). The PKC Isoform Antibody Sampler Kit (#9960), pan-phospho Ser660-PKC (#9371); AMPK and ACC Antibody Sampler Kit (#9957), anti-PSA antibody (#2475) were purchased from Cell Signaling Technology (Danvers, MA, USA). Peroxidase-conjugated antibodies against AR (sc-815) and against actin (sc-47778) were obtained from Santa Cruz Biotechnology (Santa Cruz, CA, USA).

Synthesis of 2,3-dimethoxy-1,4-naphthoquinone (DMNQ)

0.01 mol of 2,3-dichloro-1,4-naphthoquinone and 0.03 mol of sodium methoxide were refluxed in 50 ml of anhydrous methanol for 4h. At that time 0.02 mol of sodium methoxide was added to the reaction and the mixture was refluxed for 1h. The reaction product was concentrated under vacuum and the solid residue was filtered off and extensively washed with water. Yellow solid, **UV-VIS** (MeOH) λ_{\max} (nm) (ϵ_{\max} , dm³.mol⁻¹.cm⁻¹): 247 (20,200), 276 (13,700), 330 (2,800). **¹H NMR** (500 MHz, DMSO-*d*₆), δ , ppm: 7.96 (dd, *J* = 5.7, 3.3 Hz, 2H), 7.84 – 7.79 (m, 2H), 3.99 (s, 6H). **ESI-MS**, *m/z*: 241.1 [M+Na]⁺.

Synthesis of 5-O-acetylplumbagin (6-methyl-5,8-dioxo-5,8-dihydronaphthalen-1-yl acetate)

1 mmol of plumbagin in 10 ml of dichloromethane was mixed with 3 mmol of pyridine at 0°C and 2 mmol of acetyl chloride was added while mixture was stirred at 0°C. The reaction mixture was incubated for 4 h at room temperature then washed with water and brine. The dried organic phase was then resolved by column chromatography on silica to yield product. Yellow solid, **mp** 118-120°C. **UV-VIS** (MeOH) λ_{\max} (nm) (ϵ_{\max} , dm³.mol⁻¹.cm⁻¹): 245 (13,800), 252 (13,500), 337 (2,600). **¹H NMR** (500 MHz, DMSO-*d*₆), δ , ppm: 7.97 (dd, *J* = 7.7, 1.3 Hz, 1H), 7.88 (t, *J* = 7.9 Hz, 1H), 7.56 (dd, *J* = 8.0, 1.3 Hz, 1H), 6.85 (q, *J* = 1.5 Hz, 1H), 2.35 (s, 3H), 2.09 (s, 3H). **ESI-MS**, *m/z*: 253.2 [M+Na]⁺.

Formation of the plumbagin-albumin conjugate

Plumbagin was incubated with bovine serum albumin (BSA) or human serum albumin (HSA) in equimolar ratio in phosphate-buffered saline (PBS) pH7.4, for 18h at 37°C. The concentration of bound and free plumbagin was determined UV-VIS spectrophotometry (DU-640, Beckam Coulter) after chloroform extraction. The conjugate was dialyzed against PBS for 24h (Spectra/Por 12-14kDa MWCO, Spectrumlabs) and then concentrated by membrane ultrafiltration (Millipore MWCO10K).

The final concentration of albumin was determined using a BCA kit according to manufacturer's instructions (Pierce).

Cyclic voltammetry

Cyclic voltammetry measurements were performed using a computer-controlled Autolab potentiostat PGSTAT-101 (Metrohm Autolab B. V., Netherlands) and NOVA software (Metrohm Autolab B. V.). All experiments were conducted at 25°C in a conventional three-electrode cell that consisted of a glassy carbon working electrode (diameter 3 mm), a platinum wire as auxiliary electrode, and an Ag/AgCl/KCl(sat) reference electrode. The surface of the glassy carbon electrode was polished with 0.3 µm alumina powder and extensively rinsed with deionized water to obtain clean electrode surface before each measurement. Before all measurements, the cell was purged with high-purity argon. Measurements were performed at scan rate 100 mV/s.

Recovery of plumbagin, warfarin and plumbagin analogues from serum albumin

Plumbagin (10 and 100 µmol/L), warfarin (100 µmol/L), or various 1,4-naphthoquinones (100 µmol/L: juglone, naphthazarin, 1,4-naphthoquinone, menadione, 5-O-acetylplumbagin, 2,3-dimethyl-1,4-naphthoquinone and 2,3-dimethoxy-1,4-naphthoquinone), were incubated with BSA (45 mg/ml in PBS, pH7.4) at 37°C. Four replicate samples were collected from each mixture of drug/albumin at designed time-points and used for extraction. Briefly, 0.4 ml of sample was extracted with equal volume of chloroform by constant mixing at room temperature for 2 min using a vortex. Then, equal volume of trichloroacetic acid (20% v/v) was added to each sample and the mixture was mixed for 2 min. Samples were centrifuged for 5 min at 12,000 rpm. 0.1 ml aliquots of chloroform layer were evaporated. Solid residues were dissolved in 0.2 ml of methanol. The concentration of a particular drug was determined using UV-VIS spectrophotometry (DU-640, Beckam Coulter) at its respective absorption peak; UV-VIS (MeOH) λ_{\max} (nm) (ϵ_{\max} , $\text{dm}^3 \cdot \text{mol}^{-1} \cdot \text{cm}^{-1}$): plumbagin, 262 (11,800); warfarin, 304 (8,750); juglone, 246 (10,900); naphthazarin, 267 (5,080); 1,4-naphthoquinone, 242 (18,170); 5-O-acetylplumbagin, 245 (13,800); 2,3-dimethyl-1,4-naphthoquinone, 329 (14,700); 2,3-dimethoxy-1,4-naphthoquinone, 247 (20,200)). Data were normalized to initial concentration and expressed as means with corresponding Standard Deviations.

Cells

PTEN-P2 mouse prostate cancer cells generously provided by Dr. Wu [24] were grown in phenol red-free DMEM medium containing 10% heat-inactivated fetal bovine serum (FBS), 2 mmol/L L-

glutamine, 100 U/ml penicillin/100 µg/ml streptomycin and DHT 10^{-8} mol/L final. Human cancer cells LNCaP (prostate), DU145 (prostate) and UM-UC-3 (bladder) were purchased from ATCC (American Tissue Culture Collection, Manassas, VA, USA). LNCaP cells were grown in phenol-free RPMI-1640 medium containing 10% FBS, 4.5 g/l glucose and DHT 10^{-8} mol/L final. DU145 and UM-UC-3 cells were grown in DMEM containing 10% FBS, 2 mmol/L L-glutamine and 100 U/ml penicillin/100 µg/ml streptomycin. Cells were maintained in a humidified incubator at 37°C and 5% CO₂.

Cell line integrity

To prevent cell line derivation, cells were cultured for a maximum of 20 passages and started over periodically from vials frozen at very early passages. All cell lines were preemptively treated with an antimycoplasma reagent (MP Bio, Santa Ana, CA) upon arrival and at each start from a frozen vial. A mycoplasma-detection assay (Lonza, Allendale, NJ) performed at the end of the study indicated that the cells were free of mycoplasma. AR-positive prostate cancer cells PTEN-P2 and LNCaP cells have distinctive characteristics that are verified periodically (response to androgen and AR expression; LNCaP cells are also PTEN-negative).

Cell growth/viability assay

Cells were plated at a density of 5,000 cells/well in 96-well plates in normal growth medium the day before treatment. Increasing concentrations of plumbagin-albumin conjugate, up to 20 µmol/L (plumbagin equivalent) were added to the cells for 24hrs. A mass equivalent concentration of serum albumin was used as control. Cell numbers were assessed by adding 10 µL of WST-1 reagent (water soluble tetrazolium assay (2-(4-iodophenyl)-3-(4-nitrophenyl)-5-(2,4-disulfophenyl)-2H-tetrazolium; Takara).—After 90 min the optical density (OD) was measured at 430nm in a spectrophotometer (Molecular Devices; Spectra Max 250). The blank was measured from wells that did not contain cells and subtracted from all readings.

To assess the effect of plumbagin-albumin on cell growth over time, PTEN-P2 cells were treated with plumbagin-BSA and cell numbers/viability were determined daily over a period of 6 days using the WST1 assay. The culture medium was changed every other day. In one set of conditions plumbagin-albumin was added only at Day 0 (acute treatment), whereas in another set of conditions BSA control or Plumbagin-BSA were added every day (chronic treatment).

Cell cycle analysis

PTEN-P2 cells were treated with plumbagin-BSA (10 $\mu\text{mol/L}$) or with control unconjugated BSA (equivalent mass concentration) for 24, 48 and 72 hours. Attached cells were suspended with trypsin and pooled with floating cells potentially present in the medium. After two washes in PBS, cells were fixed by adding ice-cold ethanol dropwise to reach a final concentration of 70% ethanol and were maintained at 4°C for a minimum of 2hrs. Fixed cells were washed twice with PBS and suspended in PBS containing 0.1% Triton-X100 (v/v), 50 $\mu\text{g/ml}$ Propidium Iodide and 50 $\mu\text{g/ml}$ DNase-free RNase, for 30 min at 22°C. Fluorescence of single cells was measured by Flow Cytometry using the 488 nm laser on an Accuri C6 instrument (BD Biosciences, Franklin Lakes, NJ). De NovoTM FCS express Software was used for data analysis. Of note, very few apoptotic cells were seen in the pre-G1 fraction which contains fragmented DNA and were not included in the analysis.

Western blots

Cells were lysed on ice in RIPA buffer containing phosphatase and protease inhibitors as described [25]. Lysates were clarified by centrifugation for 15min at 13,000rpm, protein concentration was determined using the BCA assay (Pierce, Rockford, IL), and lysates were resuspended in SDS-PAGE buffer. After SDS-PAGE electrophoresis, proteins were transferred to Immobilon-P® membranes (Millipore, Billerica, MA). Membranes were incubated with a 5% bovine serum albumin blocking buffer for 30 min and the first antibody was incubated overnight at 4°C. Peroxidase-conjugated antibodies (Amersham Biosciences, Piscataway, NJ) were added for 45 min at 22°C followed by a 5 min incubation in Western blot LuminataTM HRP substrate (Millipore). Analysis and quantification were performed using a FluoChemTM instrument 8900 (AlphaInnotech/Protein Simple, Santa Clara, CA) Membranes were stripped using RestoreTM Stripping Buffer (Pierce/Thermo Scientific, Pittsburg, PA) for 30 min at 22°C, then reprobed with the indicated antibodies. Where indicated, results were quantified using the instrument integrated quantification software (AlphaEase FC).

RESULTS

An analysis of the cell culture parameters that influence the anti-proliferative action of plumbagin revealed that the presence of serum in the medium had a significant impact on the effect of the drug, as shown in Supplementary Figure S1. Furthermore, pre-incubation of plumbagin with serum before exposure to cells altered the pattern of anti-proliferative activity of the drug, indicating another mode of action of plumbagin when pre-exposed to serum components (Supplementary Figure S2). This correlates with the observation that plumbagin could not be recovered after 1h of incubation with serum, indicating formation of adducts with a constituent of the serum (Supplementary Figure S3). The high reactivity of the drug towards nucleophiles, the observation that it is rapidly sequestered from the serum, together with its fast clearance from the blood *in vivo* all suggest that plumbagin reacts with nucleophiles in the serum such as albumin. This prompted us to analyze the interaction of plumbagin and its analogs with albumin and to test the hypothesis that plumbagin exerts anti-cancer effects through a plumbagin-albumin adduct.

Spectral and electrochemical changes induced by interaction of plumbagin with serum albumin

UV-VIS absorption spectroscopy was used to monitor spectral changes following the addition of plumbagin to bovine serum albumin. The reference light absorption spectra of equivalent concentrations of plumbagin, DMNQ and BSA are shown in **Figure 1C**. As shown in **Figure 1Da**, a time-dependent decrease of absorption maxima corresponding to the peak absorption of plumbagin (418 nm) and a concomitant increase of absorption in the near UV range at 350-380 nm demonstrated the formation of a conjugate between plumbagin and albumin, starting immediately upon mixing with tendency to plateau at about 3 hours of incubation. On the contrary, there were no spectral changes observed over time (>30 sec) after initial addition of structural analog of plumbagin, 2,3-dimethoxy-1,4-naphthoquinone (DMNQ) to BSA (**Figure 1Db**). These results indicate that DMNQ in BSA established a rapid equilibrium of non-covalent interaction while formation of plumbagin-BSA adduct proceeded over the course of 2-3 hours.

Changes in the electrochemical activity of plumbagin upon addition to albumin are shown in **Figure 2**. Electrochemical activity was measured using cyclic voltammetry on a glassy carbon electrode in PBS as supporting electrolyte. The reference cyclic voltammograms of plumbagin in PBS showed one-peak single-step redox waves (**Figure 2A**) with reduction peaks at -0.290 V and oxidation peaks at -0.260 V (vs Ag/AgCl at scan rate 100 mV/s), indicating a two-electron redox process that is characteristic of 1,4-naphthoquinones in aqueous media [26]. The redox peak currents were proportional to the

concentration of plumbagin (**Figure 2B**). These characteristics enable us to monitor the electrochemistry and concentration of free plumbagin in aqueous solution. Electrochemical analysis of plumbagin upon addition to BSA shows an instant decrease in redox peak currents (**Figure 2C**). Gradually over time plumbagin in the BSA solution became electro-inactive, showing a complete decrease in redox peak currents to the capacitive level (**Figure 2D**). On the other hand, structural analog of plumbagin, DMNQ, did not become electrochemically inactive (**Figure 2E-F**) and after initial equilibrium (<30 sec) retained redox activity (**Figure 2F**). Changes in peak anodic current over time for plumbagin and DMNQ incubated with BSA are shown in **Figure 2G**. These results point to the formation of a supramolecular adduct of plumbagin with albumin within which the 1,4-naphthoquinone moiety of plumbagin is inaccessible for electron transfer.

To further analyze the interaction of plumbagin with albumin we investigated extraction recovery (amount of free drug that could be recovered from the complex by chloroform extraction) of plumbagin and several 1,4-naphthoquinone analogs from solutions of albumin (**Figure 3**). Warfarin, a drug known to bind non-covalently to albumin, was used to validate the extraction method. Warfarin instantly bound to albumin as evidenced by the low percentage of free warfarin recovered by membrane ultrafiltration (**Figure 3A**). As shown in **Figure 3B**, 100% of albumin-bound warfarin was recovered by chloroform extraction at all time points, consistent with the expectation that warfarin dissociates from the complex upon extraction since binding is reversible. On the other hand, the amount of free plumbagin that could be extracted from the albumin complex decreased to 0% within 2 hours of incubation, with half-lives of 15.7 min (10 $\mu\text{mol/L}$) and 18.1 min (100 $\mu\text{mol/L}$) when incubated in BSA (**Figure 3C**), and a half-life of 32.1 min when mixed with HSA (**Supplemental Figure S4**), indicative of adduct formation. These results indicate that the interaction between plumbagin and serum albumin is irreversible.

The structure-binding relationship of plumbagin and some of its analogs was analyzed to identify functional group(s) of plumbagin involved in adduct formation with albumin. A series of 1,4-naphthoquinone derivatives (juglone, naphthazarin, 1,4-naphthoquinone, menadione, 2,3-dimethyl-1,4-naphthoquinone) were acquired from a commercial source, whereas 5-O-acetyl-plumbagin and 2,3-dimethoxy-1,4-naphthoquinone were synthesized as described in Methods. The chemical structure of each drug used in these experiments is shown in **Figure 3D**. Each analog was mixed with albumin and the amount of analog that could be extracted by the chloroform method was determined by UV-VIS spectrophotometry. As shown in **Figure 3E**, Plumbagin, juglone, naphthazarin, 1,4-naphthoquinone,

menadione and 5-O-acetyl-plumbagin were not extractible from the albumin complex (<1%) but showed almost complete retention after 18 hours of incubation with albumin. On the other hand, plumbagin analogs 2,3-dimethoxy-1,4-naphthoquinone and 2,3-dimethyl-1,4-naphthoquinone were completely recovered by extraction, indicating that they did not form an irreversible adduct with albumin. Thus, 1,4-naphthoquinones with at least one unsubstituted quinoid carbon (C-2 or C-3) can irreversibly bind to serum albumin, presumably through covalent bond, whereas 1,4-naphthoquinones with substituted quinoid carbons (both C-2 and C-3) do not form irreversible adducts with serum albumin. These results indicate the site-specific nucleophilic addition of serum albumin to the C-2 or C-3 carbon of plumbagin.

Biological effect of plumbagin-albumin

To ascertain the biological activity of the adduct and its potential contribution to the effects of plumbagin on the growth of tumor cells *in vitro*, plumbagin-albumin was added to cancer cells and cell numbers were evaluated 24h later using the WST-1 assay. As shown in **Figure 4A**, the plumbagin-BSA adduct caused a dose-dependent growth inhibition in mouse prostate cancer cells PTEN-P2. No effect of plumbagin-BSA was observed in human prostate cancer cells DU145, whereas plumbagin-HSA decreased their growth, suggesting that cellular effects of the conjugate are species-specific. Plumbagin-HSA also inhibited the growth of human bladder cancer cells UM-UC-3 (**Figure 4A**) and of human breast cancer cells MCF-7 (data not shown). This species specific effect of the plumbagin-serum albumin adduct suggests that it is mediated via cell surface receptor-mediated endocytosis. Various albumin-binding receptors have been identified in human cells including cancer cells (reviewed in [22]). Since bovine and murine albumin share high sequence homology, plumbagin-BSA is expected to interact with mouse cells, whereas there is only about 70% homology between bovine and human albumin, explaining that only the plumbagin-HSA conjugate was active in human cells. The receptor/albumin-plumbagin complex is then internalized by receptor-mediated endocytosis. While the receptor is recycled, albumin is subject to lysosomal degradation (reviewed in [27, 28]). To test whether lysosomal degradation is necessary, we used various protease inhibitors including pepstatin A, which inhibits lysosomal proteases cathepsins D and E. Thus, serine protease inhibitor leupeptin, caspase inhibitor Z-VAD, pepsin and cathepsin D/E inhibitor Pepstatin A, and anti-oxidant Trolox were pre-incubated with cancer cells before addition of plumbagin-BSA or BSA control. Twenty-four hours later cell proliferation was evaluated by WST1. As shown in **Figure 4B**, plumbagin-BSA inhibited cell growth by 50% following a 24h incubation. Leupeptin, Z-VAD and

trolox did not influence this effect, whereas pepstatin A antagonized the effect of plumbagin-albumin, indicating that lysosomal degradation is necessary for the biological activity of the adduct. Of note, earlier experiments have shown that pepstatin A does not antagonize the effect of free plumbagin (**Supplementary Figure S5**).

The observation that plumbagin-albumin fails to inhibit cell growth in cells pre-treated with pepstatin A supports the hypothesis that processing of albumin-plumbagin adduct by lysosomal degradation is necessary for release of the active form of plumbagin. Thus, we hypothesize that following receptor-mediated internalization and proteolytic degradation of plumbagin-albumin adduct in lysosomes, the amino acid/peptide-adducts of plumbagin are released into the cytosol, essentially resulting in the post-catabolic release of a small plumbagin adduct in which plumbagin is accessible, in contrast to the large intact plumbagin-albumin adduct in which plumbagin is “protected” within the binding pocket. Small molecule 1,4-naphthoquinone adducts such as the cysteine-plumbagin adduct have been shown to be redox-active with the same potential range of action as plumbagin [29]. Therefore these very small adducts are capable of redox cycling to form ROS species and are expected to exert similar anti-proliferative activity as free plumbagin. On the other hand, digested plumbagin-albumin adducts could possibly undergo a retro-Michael reaction that would liberate free plumbagin. This will be the subject of future research aimed at providing more insight into the mechanism of action of the plumbagin-albumin adduct discovered here.

Plumbagin conjugated with serum albumin did not obviously alter cell morphology, although there were noticeably fewer cells after plumbagin treatment for 24h than in the control, which is consistent with an effect on cell growth (**Supplementary Figure S6**). Of note, the morphology of cells incubated with free plumbagin was markedly different, with early evidence of catastrophic cell death not visible in the presence of plumbagin-albumin. In addition, the morphology of cells treated with the adduct was very similar to conditions in which plumbagin was quenched by serum (**Supplementary Figures S1 and S2**).

When cell growth was measured over time, it was observed that the adduct completely inhibited cell growth compared to control-treated cells, as shown in **Figure 5A**. It is interesting to note that the effect of an acute one-time treatment with plumbagin-albumin adduct caused growth inhibition for as long as 3 days, suggesting a long half-life of the adduct *in vitro*. The inhibition was reversible because cells started growing again 4 days after the one-time treatment. Chronic exposure, on the other hand, led to

prolonged and complete inhibition of cell growth and eventually to some cell death, since the number of cells at day 6 was half of the number of plated cells ($4,939 \pm 570$ initial versus $2,695 \pm 400$ at day 6).

To evaluate the effect of plumbagin-albumin adduct on cell cycle progression, non-synchronized PTEN-P2 cells growing in normal culture medium were treated with either un-conjugated BSA or plumbagin-BSA for the indicated times. Cells were stained with propidium iodide for flow cytometry analysis. The proportion of cells in each phase of the cell cycle did not vary significantly as a function of time when cells were treated with control BSA and a classic pattern of phase distribution was observed in which phase G1 was predominant and accounted for approximately 50% of the cells (**Figure 5B and C**). About 25% of cells were in S phase, as expected from a non-synchronized, actively growing cell population. It was observed that the proportion of cells in G1 phase decreased upon treatment with plumbagin-BSA adduct, while the proportion of cells in S phase and G2/M increased. These results indicate that plumbagin-BSA adduct alters cell cycle progression and are consistent with a depletion of the cells in G1 and a block in the G2/M phase, either at the G2 checkpoint or in mitosis.

To determine if the effect on the cell cycle could be explained by alterations in the expression or phosphorylation levels of cell cycle regulators, PTEN-P2 cells were treated with plumbagin-BSA adduct at increasing concentrations and for variable periods of time. Expression and phosphorylation levels of cell cycle proteins were analyzed by western blot. Few cell cycle regulators were affected by plumbagin-BSA adduct. For example, no alteration was observed in cyclin D1, p27^{KIP1}, p21^{CIP1}, p19^{INK4d}, CDK1/cdc2, among others (not shown). However, plumbagin-albumin decreased protein levels of p48-RBBP protein isoforms by $\geq 80\%$ (**Figure 5D**).

On the other hand, the plumbagin-albumin adduct did not activate tumor suppressor p53 and did not induce p21^{CIP1} in PTEN-P2 cancer cells, which was similar to the lack of effect observed in response to free plumbagin (**Supplementary Figure S7**).

We have shown previously that in prostate cancer cells, plumbagin decreases the protein expression of the androgen receptor (AR) [9] and decreases the hormone-induced expression of AR target genes [30]. This is particularly relevant to the effect of plumbagin in prostate cancer because prostate tumors depend on the AR axis for growth. When AR-positive prostate cancer cells PTEN-P2 were treated with plumbagin-BSA, a dose-dependent decrease in AR protein levels was observed (**Figure 6A**). The effect peaked at 5 $\mu\text{mol/L}$ (**Figure 6A**) after 16 hours of treatment and lasted at least 24h following single treatment (**Figure 6B**). The average AR expression following treatment with 10 $\mu\text{mol/L}$ of

plumbagin conjugate for 24h was $34\% \pm 4.5$ of control and was statistically significant ($p=0.0028$, t-test, **Figure 6C**). Consistently, exposure to plumbagin-albumin adduct also decreased the expression of AR target protein PSA (prostate specific antigen) in human prostate cancer cells LNCaP (**Figure 6D**).

It was also observed that plumbagin-albumin adduct caused a decrease in the protein levels of various PKC isoforms, including protein levels of PKC ϵ , thereby mimicking the well described effect of plumbagin on prostate tumors in animals [6, 31-33]. The effect of plumbagin-albumin on PKC levels was analyzed by treating cells with plumbagin-albumin, followed by western blot analysis. As shown in **Figure 7A**, the conjugate decreased the protein expression levels of PKC ϵ , PKC μ and PKC δ with a maximum effect at 24h. Average PKC ϵ expression following treatment with $10 \mu\text{mol/L}$ of plumbagin conjugate for 24h was 36.8% of control ($\text{SE} \pm 5.0$) and was statistically significant ($p=0.0026$, **Figure 7B**). Of note, PKC α and PKC ζ were not detectable by western blot in these cells. **Figure 7C** shows that treatment with plumbagin-albumin caused a partial decrease in the phosphorylation of PKC (measured using a pan-antibody), which is likely a result of the decreased expression of the corresponding isoform.

Interestingly, the conjugate stimulated the phosphorylation of AMPK α and the phosphorylation of AMPK α direct target ACC (acetyl-CoA carboxylase). The average AMPK α phosphorylation following treatment with $10 \mu\text{mol/L}$ of plumbagin conjugate for 1h was increased 4 fold ($p=0.03$, **Figure 7D**). Because activation of AMPK α is another known effect of free plumbagin [34, 35], these results also suggest that the conjugate has similar biological effects as unconjugated plumbagin.

We conclude that the plumbagin-albumin adduct mimics at least some of the cellular effects of plumbagin including known *in vivo* molecular alterations and therefore is biologically relevant.

DISCUSSION

Serum albumin is the most abundant protein in the plasma (35 - 50 g/L). It binds to a wide range of drugs, limiting their free concentration and altering their metabolism, distribution and physiological effects. This can be desirable as it may, for instance, increase the solubility of an otherwise poorly soluble drug, slow its distribution through the organism, and increase its half-life while decreasing its side-effects. Albumin therefore has emerged as a potential carrier for therapeutic drugs and several drug delivery systems that effectively exploits albumin as a drug carrier have entered clinical trials or are used clinically [15, 36].

Several therapeutics or their reactive metabolites form covalent complexes with serum albumin, including BI-94 [37] and Neratinib (HKI-272) [38] among others. These typically include soft electrophiles such as α,β -unsaturated carbonyl compounds, quinones, quinone imines, quinone methides, imine methide, isocyanate, isothiocyanates, aziridinium, etc [39, 40]. The soft electrophiles react with cysteine residues in proteins acting as soft nucleophilic substrates [39, 41]. Serum albumin contains a free accessible cysteine residue (Cys-34) [42-44]. The free thiol group of Cys-34 is very reactive toward electrophiles at physiological pH due to low pKa value of 6.5 [45]. In plasma, free thiol at Cys-34 of serum albumin (0.5 - 0.8 mM) is the most abundant thiol [46] and as such it is expected to act as a trap for soft electrophiles.

1,4-naphthoquinones including plumbagin are highly reactive organic chemical species toward biological nucleophiles [47]. Added to the observation that the effect of plumbagin is rapidly altered by serum in cell culture medium, together with its fast clearance from the blood *in vivo* [11, 12], all suggest that plumbagin rapidly reacts with endogenous nucleophiles abundant in the serum such as albumin. Indeed, plumbagin and structurally related 1,4-naphthoquinones with at least one unsubstituted quinoid carbon (C2 or C3) showed instantaneous formation of supramolecular adduct with of albumin as supported by extraction recovery experiments. Necessity for the unsubstituted carbon in 1,4-naphthoquinone core indicates binding via Michael's addition reaction, where plumbagin and other 1,4-naphthoquinones being α, β -unsaturated diketones act as electrophilic acceptors in 1,4-addition reaction [47]. These findings support the hypothesis that plumbagin forms covalent adduct with albumin, most likely through a cysteine residue such as free Cys-34.

Furthermore, it is hypothesized that the adduct specifically interacts with cells via a cell surface receptor for albumin that is internalized and degraded in the lysosomes, thus releasing the active form of plumbagin. The plumbagin-albumin adduct profoundly inhibited cell growth and caused cell cycle

arrest. The adduct is biologically relevant and represents a credible intermediary *in vivo*, as it showed similar cellular effects as have been described for free plumbagin. For instance, the plumbagin-albumin adduct inhibited cell growth through cell cycle arrest in the G2/M phase. We observed that plumbagin-albumin did not activate the p53/p21^{CIP} pathway but reduced the expression of RBBP family of proteins. RBBP family of proteins are retinoblastoma-binding proteins with histone or DNA-binding capabilities, functioning as cofactors and regulators of chromatin assembly factors, chromatin remodeling factors and histone modification enzymes. They play a crucial role in DNA replication and as cell cycle checkpoints, and therefore in the control of cell proliferation.

We then looked at pertinent cellular responses, the first of which is the well documented decrease in the expression of PKC- ϵ *in vivo*. Thus, plumbagin consistently reduced the expression of PKC- ϵ in the tumors of treated animals compared to non-treated animals in various mouse models of prostate cancer (Aziz et al., 2008; Hafeez et al., 2013; Hafeez et al., 2012). It is noteworthy that different routes of administration (intra-peritoneal and per oral) tested in various models resulted in similar effects. In addition, the very consistent decrease of PKC- ϵ levels in plumbagin-treated tumors points to this kinase as a crucial target. PKC- ϵ is a master switch regulator of cell signaling that regulates cancer-relevant biological functions such as differentiation and proliferation, and therefore may play an important role in the anti-cancer effect of plumbagin. Its expression is often altered in prostate tumors, in which it appears to act as an oncogene (reviewed in [48, 49]). Recent studies have also shown that it may be involved in prostate cancer metastasis [50]. A second target of plumbagin that is especially pertinent to prostate cancer, for which plumbagin is in clinical trial, is the androgen receptor. Plumbagin has been shown previously to inhibit AR expression [9] and to decrease the hormone-induced expression of AR target genes [30]. It is shown here that plumbagin-BSA indeed decreased AR expression in PTEN-P2 prostate cancer cells. In addition, plumbagin-HSA decreased the AR target PSA in LNCaP human prostate cancer cells. Prostate tumors depend on AR signaling for growth, therefore the observation that plumbagin-albumin has a similar inhibitory effect on AR as unconjugated plumbagin is physiologically relevant. Finally, plumbagin-albumin increased the phosphorylation of AMPK α and its direct target ACC, a similar effect as described previously for plumbagin [34, 35]. AMPK is an evolutionarily conserved serine/threonine kinase that functions as a sensor of cellular energy levels and regulates metabolism. In particular, AMPK stimulates glycolysis and increases glucose uptake, inhibits glycogen synthesis and overall regulates glucose metabolism. It also inhibits protein synthesis, activates autophagy, and decreases lipid anabolism while activating

lipid catabolism [51]. Thus, activation of AMPK is known to contribute to the anti-cancer properties of several drugs such as metformin and is relevant to the anti-cancer effect of plumbagin.

The interaction between serum albumin and drug is therefore an important factor to consider during the development of a new therapeutic [17]. The spontaneous plumbagin-albumin adduct described here involves the formation of a covalent, stable bond possibly between cysteine 34 of albumin and carbon C3 of plumbagin. Our finding is consistent with the long-known reactivity of 2-methyl-1,4-naphthoquinones with sulfhydryl groups and cysteine, which involves the 3-position on the quinone ring [52, 53]. The thiolate group of cysteine-34 in human serum albumin is reactive under physiological pH because of its low pKa (~6.5) [45, 54]. It is therefore exploited to conjugate drugs to albumin as a means of delivery (reviewed in [55]). Considering the high reactivity of plumbagin toward cysteine and cysteine-containing nucleophiles, together with the presence of a free cysteine residue in serum albumin in physiological conditions, the formation of the plumbagin-albumin adduct is expected. Previous reports have described the binding of naphthoquinones with cysteine in albumin and, most importantly, their detection *in vivo*. For example, treatment of rats with naphthalene induced cysteinyl adducts of both hemoglobin and albumin with naphthalene metabolites 1,2-naphthoquinone and 1,4-naphthoquinone in a dose-dependent manner [56] whereas serum albumin adducts of both 1,2-naphthoquinone and 1,4-naphthoquinone metabolites have been detected in the blood of human subjects [57].

Overall, the binding of plumbagin to serum albumin naturally solves the problems of plumbagin's poor aqueous solubility, high lipophilicity and instability (reactivity), which were thought likely to impede its clinical translation by limiting its bioavailability, *in vivo* absorption, distribution and tumor uptake. Indeed, many laboratories, including ours [58], have designed new formulations and delivery systems such as liposomes, niosomes, microspheres, nanoparticles, micelles, complexation, metal nanoparticles, crystals modification, etc (reviewed in [59]). Our new findings suggest that these efforts may be unnecessary if conjugation to albumin improves the pharmacokinetic profile of plumbagin. In agreement with this notion, we observed that despite its rapid clearance in plasma, plumbagin displayed long-lasting effects *in vivo*. A mouse prostate tumor model was used to compare several plumbagin administration schedules as previously described [8, 9]. As shown in **Supplementary Figure S8**, and consistent with previous findings, per oral plumbagin at 1mg/kg caused tumors to shrink over time. Similar efficacy was observed when plumbagin was administered once/day, every 3 days or every 5 days, whereas administration every 7 days was less efficient at decreasing tumor size

than other schedules. This experiment indicates that plumbagin *in vivo* has prolonged effects, in apparent contradiction with its fast clearance from plasma.

Accumulation of albumin in tumors makes it particularly appealing for oncology drug development [60, 61] and represents a particularly relevant property considering that plumbagin will be used as an anti-cancer agent. There are several passive and active mechanisms that facilitate the accumulation of albumin in solid tumors, particularly enhanced permeability and retention (EPR) of macromolecules in tumor tissue due to leaky tumor blood vessels and a lack of lymphatic drainage [19, 20]. Furthermore, albumin-binding proteins such as albondin (gp 60) expressed on the endothelial cell surface and SPARC (Secreted Protein, Acidic and Rich in Cysteine) present in the tumor interstitium facilitate the uptake and retention of albumin in the tumor interstitium [14, 22]. Albumin also accumulates in tumors because of high metabolic turnover associated with hypoalbuminaemia in patients with advanced solid tumors [62].

In summary, plumbagin-albumin adducts are hypothesized to naturally take advantage of the desirable properties of human serum albumin, such as better solubility, increased accumulation in tumors, increased plasma half-life of small molecule drugs, and reduced toxicity. Spontaneous formation of a plumbagin-albumin adduct as described here explains the rapid clearance of plumbagin from plasma upon administration. When added to cancer cells the conjugate displayed several cellular effects consistent with known action of plumbagin such as cell growth inhibition, cell cycle arrest, decreased expression of AR and PKC isoforms, increased AMPK phosphorylation, and therefore represents a biologically relevant intermediate of plumbagin.

REFERENCES

1. S. Padhye, P. Dandawate, M. Yusufi, A. Ahmad, F.H. Sarkar. *Med. Res. Rev.* 2012, **32**: 1131-1158.
2. P. Panichayupakaranant, M.I. Ahmad. *Adv. Exp. Med. Biol.* 2016, **929**: 229-246.
3. Y. Liu, Y. Cai, C. He, M. Chen, H. Li. *Am. J. Chin. Med.* 2017, **45**: 423-441.
4. S.K. Tripathi, M. Panda, B.K. Biswal. *Food Chem. Toxicol.* 2019, **125**: 566-582.
5. W. Yan, T.Y. Wang, Q.M. Fan, L. Du, J.K. Xu, Z.J. Zhai, H.W. Li, T.T. Tang. *Acta. Pharmacol. Sin.* 2014, **35**(1): 124-134.
6. B.B. Hafeez, W. Zhong, J.W. Fischer, A. Mustafa, X. Shi, L. Meske, H. Hong, W. Cai, T. Havighurst, K. Kim, A.K. Verma. *Mol. Oncol.* 2013, **7**: 428-439.
7. C.G. Kang, E. Im, H.J. Lee, E.O. Lee. *Bioorg. Med. Chem. Lett.* 2017, **27**: 1914-1918.
8. P. Abedinpour, V.T. Baron, A. Chrastina, J. Welsh, P. Borgström, *Prostate* 2013, **73**: 489-99.
9. P. Abedinpour, V.T. Baron, A. Chrastina, G. Rondeau, J. Pelayo, J. Welsh, P. Borgström, *Prostate* 2017, **77**: 1550-1562.
10. C. Kyriakopoulos, C.J. Paller, A. Verma, K. Kader, J. Kittrelle, P. Borgström, U.N. Vaishampayan. *Journal of Clinical Oncology* 2019, **37**: 15_suppl, e16517-e16517.
11. M.R. Kumar, B.K. Aithal, N. Udupa, M.S. Reddy, V. Raakesh, R.S. Murthy, D.P. Raju, B.S. Rao. *Drug Deliv.* 2011, **18**: 511-522.
12. Y.J. Hsieh, L.C. Lin, T.H. Tsai. *J. Chromatogr. B. Analyt. Technol. Biomed. Life Sci.* 2006, **844**(1): 1-5.
13. B.R. Jali, Y. Kuang, N. Neamati, J.B. Baruah. *Chem. Biol. Interact.* 2014, **214**: 10-17.
14. F. Kratz. *J. Control Release* 2014, **190**: 331-336.
15. E.N. Hoogenboezem, C.L. Duvall. *Adv. Drug Deliv. Rev.* 2018, **130**: 73-89.
16. F. Kratz, B. Elsadek. *J. Control Release* 2012, **161**(2): 429-445.
17. K. Yamasaki, V.T. Chuang, T. Maruyama, M. Otagiri. *Biochim. Biophys. Acta.* 2013, **1830**: 5435-5443.
18. D. Sleep, J. Cameron, L.R. Evans. *Biochim. Biophys. Acta.* 2013, **1830**: 5526-5534.
19. H. Maeda, J. Wu, T. Sawa, Y. Matsumura, K. Hori. *J. Control Release* 2000, **65**(1-2): 271-284.
20. A. Mukherjee, B. Kumar, K. Hatano, L.M. Russell, B.J. Trock, P.C. Searson, A.K. Meeker, M.G. Pomper, S.E. Lupold. *Mol. Cancer Ther.* 2016, **15**(10): 2541-2550.
21. J.E. Schnitzer. *Am. J. Physiol.* 1992, **262**(1 Pt 2): H246-54.
22. A.M. Merlot, D.S. Kalinowski, D.R. Richardson. *Front. Physiol.* 2014, **5**: 299.

23. J.E. Schnitzer, A. Sung, R. Horvat, J. Bravo. *J. Biol. Chem.* 1992, **267**(34): 24544-24553.
24. J. Jiao, S. Wang, R. Qiao, I. Vivanco, P.A. Watson, C.L. Sawyers, H. Wu: *Cancer Res.* 2007, **67**: 6083-6091.
25. R. Pio, Z. Jia, V.T. Baron, D. Mercola, UCI NCI SPECS. *PLoS One* 2013, **8**(1): e54096.
26. P.S. Guin, S. Das, P.C. Mandal. *Int. J. Electrochem.* 2011, **2011**: 1-22.
27. N.J. Brunskill. *Nephrol. Dial. Transplant.* 2000, **15**(11): 1732-1734.
28. E. Frei. *Diabetol. Metab. Syndr.* 2011, **3**(1):11.
29. M. Damle, L.A.A. Newton, M. M. Villalba, R. Leslie, J. Davis. *Electroanalysis* 2010, **22**(21): 2491–2495.
30. G. Rondeau, P. Abedinpour, A. Chrastina, J. Pelayo, P. Borgstrom, J. Welsh. *Sci. Rep.* 2018, **8**(1): 2694.
31. M.H. Aziz, N.E. Dreckschmidt, A.K. Verma, *Cancer Res.* 2008, **68**: 9024-9032.
32. B.B. Hafeez, W. Zhong, A. Mustafa, J.W. Fischer, O. Witkowsky, A.K. Verma. *Carcinogenesis* 2012, **33**: 2586-2592.
33. B.B. Hafeez, J.W. Fischer, A. Singh, W. Zhong, A. Mustafa, L. Meske, M.O. Sheikhani, A.K. Verma. *Cancer Prev. Res.* 2015, **8**: 375-386.
34. M.B. Chen, Y. Zhang, M.X. Wei, W. Shen, X.Y. Wu, C. Yao, P.H. Lu. *Cell Signal.* 2013, **25**: 1993-2002.
35. H. Wang, H. Zhang, Y. Zhang, D. Wang, X. Cheng, F. Yang, Q. Zhang, Z. Xue, Y. Li, L. Zhang, L. Yang, G. Miao, D. Li, Z. Guan, Y. Da, Z. Yao, F. Gao, L. Qiao, L. Kong, R. Zhang. *Oncotarget.* 2016, **7**: 82864-82875.
36. M.T. Larsen, M. Kuhlmann, M.L. Hvam, K.A. Howard. *Mol. Cell. Ther.* 2016, **4**: 3.
37. N. Gautam, R. Thakare, S. Rana, A. Natarajan, Y. Alnouti. *Xenobiotica* (2015) **45**(10): 858-873.
38. J. Wang, X.X. Li-Chan, J. Atherton, L. Deng, R. Espina, L. Yu, P. Horwatt, S. Ross, S. Lockhead, S. Ahmad, A. Chandrasekaran, A. Oganessian, J. Scatina, A. Mutlib, R. Talaat. *Drug Metab. Dispos.* 2010, **38**(7): 1083-1093.
39. C. Prakash, R. Sharma, M. Gleave, A. Nedderman. *Curr. Drug Metab.* 2008, **9**(9): 952-964.
40. W. Tang, A.Y. Lu. *Drug. Metab. Rev.* 2010, **42**(2): 225-249.
41. F. Li, J. Lu, X. Ma. *Chem. Res. Toxicol.* 2011, **24**(5): 744-751.
42. M. Sogami, S. Era, S. Nagaoka, K. Kuwata, K. Kida, J. Shigemi, K. Miura, E. Suzuki, Y. Muto, E. Tomita, et al. *J. Chromatogr.* 1985, **332**: 19-27.
43. S. Era, T. Hamaguchi, M. Sogami, K. Kuwata, E. Suzuki, K. Miura, K. Kawai, Y. Kitazawa, H. Okabe, A. Noma, et al. *Int. J. Pept. Protein Res.* 1988, **31**: 435-442.

44. T. Etoh, M. Miyazaki, K. Harada, M. Nakayama, A. Sugii. *J. Chromatogr.* 1992, **578**: 292-296.
45. A.J. Stewart, C.A. Blindauer, S. Berezenko, D. Sleep, D. Tooth, P.J. Sadler. *FEBS J.* 2005, **272**(2): 353-362.
46. L. Turell, R. Radi, B. Alvarez. *Free Radic. Biol. Med.* 2013, **65**: 244-253.
47. Y. Kumagai, Y. Shinkai, T. Miura, A.K. Cho. *Annu. Rev. Pharmacol. Toxicol.* 2012, **52**: 221-247.
48. A.S. Ali, S. Ali, B.F. El-Rayes, P.A. Philip, F.H. Sarkar. *Cancer Treat. Rev.* 2009, **35**: 1-8.
49. E. Totoń, E. Ignatowicz, K. Skrzeczkowska, M. Rybczyńska. *Pharmacol. Rep.* 2011, **63**: 19-29.
50. A. Gutierrez-Uzquiza, C. Lopez-Haber, D.L. Jernigan, A. Fatatis, M.G. Kazanietz. *Mol. Cancer Res.* 2015 **13**: 1336-1346.
51. S.M. Jeon. *Exp. Mol. Med.* 2016, **48**: e245.
52. C.A. Colwell, M. McCall. *Science* 1945, **101**(2632): 592-594.
53. L.F. Fieser, R.B. Turner. *J. Am. Chem. Soc.* 1947, **69**(10): 2335-2338.
54. A.O. Pedersen, J. Jacobsen. *Eur. J. Biochem.* 1980, **106**: 291-295.
55. M.B. Caspersen, M. Kuhlmann, K. Nicholls, M.J. Saxton, B. Andersen, K. Bunting, J. Cameron, K.A. Howard. *Ther. Deliv.* 2017, **8**(7): 511-519.
56. S. Waidyanatha, M.A. Troester, A.B. Lindstrom, S.M. Rappaport. *Chem. Biol. Interact.* 2002, **141**(3): 189-210.
57. P.H. Lin, D.R. Chen, T.W. Wang, C.H. Lin, M.C. Chuang. *Chem. Biol. Interact.* 2009, **181**(1): 107-114.
58. A. Chrastina, V.T. Baron, P. Abedinpour, G. Rondeau, J. Welsh, P. Borgström. *Biomed. Res. Int.* 2018, **2018**: 9035452.
59. S. Rajalakshmi, N. Vyawahare, A. Pawar, P. Mahaparale, B. Chellampillai. *Artif. Cells Nanomed. Biotechnol.* 2018, **46**(sup1): 209-218.
60. G. Stehle, H. Sinn, A. Wunder, H.H. Schrenk, S. Schütt, W. Maier-Borst, D.L. Heene. *Anticancer Drugs.* 1997, **8**: 677-685.
61. P. Kremer, M. Fardanesh, R. Ding, M. Pritsch, S. Zoubaa, E. Frei. *Neurosurgery* 2009, **64**: 53-60.
62. C.A. Hauser, M.R. Stockler, M.H. Tattersall. *Support. Care Cancer.* 2006, **14**(10): 999-1011.

LEGENDS

Figure 1. Spectral analysis of complex formation.

Panel A: structure of plumbagin (5-hydroxy-2-methyl-1,4-naphthoquinone). **Panel B:** structure of DMNQ (2,3-dimethoxy-1,4-naphthoquinone). **Panel C:** Reference light absorption spectra of 100 $\mu\text{mol/L}$ plumbagin, DMNQ and 4.5 % BSA (w/v) in PBS at pH7.4. The peak absorption of plumbagin was at 418 nm and the peak absorption of DMNQ was at 339 nm. **Panel D:** Spectral changes of 100 $\mu\text{mol/L}$ plumbagin (left) and 100 $\mu\text{mol/L}$ DMNQ (right) mixed with albumin were monitored at various time points (30 sec - 6h) starting immediately upon incubation with BSA (45 mg/ml) in PBS at pH7.4. UV-VIS light absorption spectra were acquired using a DU-640 spectrophotometer (Backman Coulter). Insets show the progressive decrease in absorbance at the peak absorption of plumbagin (418 nm), a change not observed at the peak absorption of DMNQ (339 nm).

Figure 2: Changes in plumbagin redox activity upon complex formation

Panel A: Concentration-dependent cyclic voltammograms of plumbagin (concentration range 0.2-100 $\mu\text{mol/L}$) in PBS at pH 7.4. Working electrode, GC, counter electrode, Pt, reference electrode, Ag/AgCl/sat, scan rate, $v=100$ mV/s. **Panel B:** Peak anodic current (I_{pa}) as a function of plumbagin concentration. **Panel C:** Time-dependent changes in the redox activity of plumbagin were measured by recording cyclic voltammograms at 10 sec, 30 min, 1 and 3 h after addition of 100 $\mu\text{mol/L}$ plumbagin to BSA (45 mg/ml) in PBS at pH 7.4. The arrows indicate the direction of time-dependent changes from 10 sec to 3 h. **Panel D:** Scaled-up CVs of plumbagin. **Panel E:** Time-dependent changes in the redox activity of 100 $\mu\text{mol/L}$ DMNQ mixed with BSA in the same conditions as plumbagin. **Panel F:** Scaled-up CVs of DMNQ. DMNQ did not show further variation in I-E profile and in redox peak currents. Experimental conditions: working electrode, GC, counter electrode, Pt, reference electrode, Ag/AgCl/sat, scan rate, $v=100$ mV/s. **Panel G:** Changes in peak anodic current (i_{pa}) over time for plumbagin and DMNQ in BSA. The i_{pa} values were determined from cyclic voltammograms of 100 $\mu\text{mol/L}$ plumbagin or DMNQ incubated with BSA, acquired at indicated time points. The dotted line (.....) shows the level of capacitive current (unconjugated BSA in PBS).

Figure 3: Extraction recovery of plumbagin and 1,4-naphthoquinone analogs to albumin.

Panel A: Warfarin was added to BSA (45 mg/ml in PBS, pH7.4, 37°C) at a final concentration of 100 $\mu\text{mol/L}$. The percentage of free warfarin and of warfarin bound to BSA as estimated by membrane ultrafiltration using Amicon Ultracell 10 K (Millipore). **Panel B:** Extraction recovery of warfarin from

albumin. Non-covalently bound warfarin was extracted by chloroform at the indicated time points. Amount of extracted drug was determined by UV-VIS spectroscopy as described in methods. The ratio of recovered (free) drug from the complex was calculated at the indicated time points. **Panel C:** Extraction recovery of plumbagin from albumin. Plumbagin was added to BSA (45 mg/ml in PBS, pH7.4, 37°C for 18h) at final concentrations of 10 and 100 $\mu\text{mol/L}$. **Panel D:** Structure of 1,4-naphthoquinones structurally related to plumbagin. Plumbagin (A), juglone (B), naphthazarin (C), 1,4-naphthoquinone (D), menadione (E), 5-Oacetyl-plumbagin (F), 2,3-dimethoxy-1,4-naphthoquinone (G) and 2,3-dimethyl-1,4-naphthoquinone (H). **Panel E:** Recovery of 1,4-naphthoquinones from BSA. Each 1,4-naphthoquinone (100 $\mu\text{mol/L}$) was incubated with BSA (45 mg/ml in PBS, pH 7.4, 37°C for 18h). Recovery indicates reversible non-covalent interaction with serum albumin, while lack of recovery demonstrates adduct formation.

Figure 4: Species specificity and lysosomal-dependency of the effect of plumbagin-albumin

Panel A: Mouse and human cancer cells were plated 24h before the experiment. Plumbagin-albumin was added at increasing concentrations up to 20 $\mu\text{mol/L}$ of plumbagin for 24h. Unconjugated BSA or HSA were used as control as appropriate (mass equivalent). Cell numbers were evaluated using the WST-1 assay. Each graph represents the means $\pm\text{SEM}$ of at least 3 independent experiments, each performed in triplicates, except for UM-UC-3 (2 independent experiment, each performed in triplicates). **Panel B:** PTEN-P2 cells were pre-incubated with or without various inhibitors for 3hrs before addition of conjugate plumbagin-BSA (10 $\mu\text{mol/L}$ plumbagin) or unconjugated BSA (equimolar to albumin adduct) for 24h. Inhibitors were: serine protease inhibitor leupeptin (125 $\mu\text{mol/L}$); caspase inhibitor Z-VAD (25 $\mu\text{mol/L}$); cathepsin D/E inhibitor pepstatin A (2.5 $\mu\text{mol/L}$); anti-oxidant Trolox (20 $\mu\text{mol/L}$). Cell numbers were evaluated using the WST-1 assay. The graph represents the means $\pm\text{SEM}$ of 3 independent experiments (n=2 for Trolox), each performed in triplicates. Results are expressed as % of control (BSA alone).

Figure 5: Effect of plumbagin-albumin on cell growth

Panel A: Growth over time of cells treated with plumbagin-albumin. Conjugated plumbagin-BSA (10 $\mu\text{mol/L}$) or BSA (mass equivalent) were added to PTEN-P2 cells at day 0 for a one-time treatment (acute treatment), or every day from day 0 (chronic treatment). The number of cells was evaluated

every day by measuring mitochondrial activity using the WST-1 assay. The graph represents the means \pm SEM of 3 separate experiments, each performed in triplicates. Results are expressed as percent of maximum as a function of time. **Panels B:** Cell cycle analysis. PTEN-P2 cells were incubated with BSA or with plumbagin-BSA for 24h, 48 and 72h. Cells were suspended, fixed and stained with propidium iodide followed by flow cytometry. Cell cycle phases were analyzed using De Novo™ FCS express. **Panel C:** The proportion of cells in each phase of the cell cycle was represented in pie charts. **Panel D:** Western blot analysis of RBBP expression following plumbagin-albumin treatment. Cells were incubated with increasing concentrations of plumbagin-BSA. After 24h, cells were lysed and the relative protein expression was analyzed by western blot. The membrane was stripped and probed again with the indicated antibodies. The insert shows the quantification of RBBP expression in this experiment.

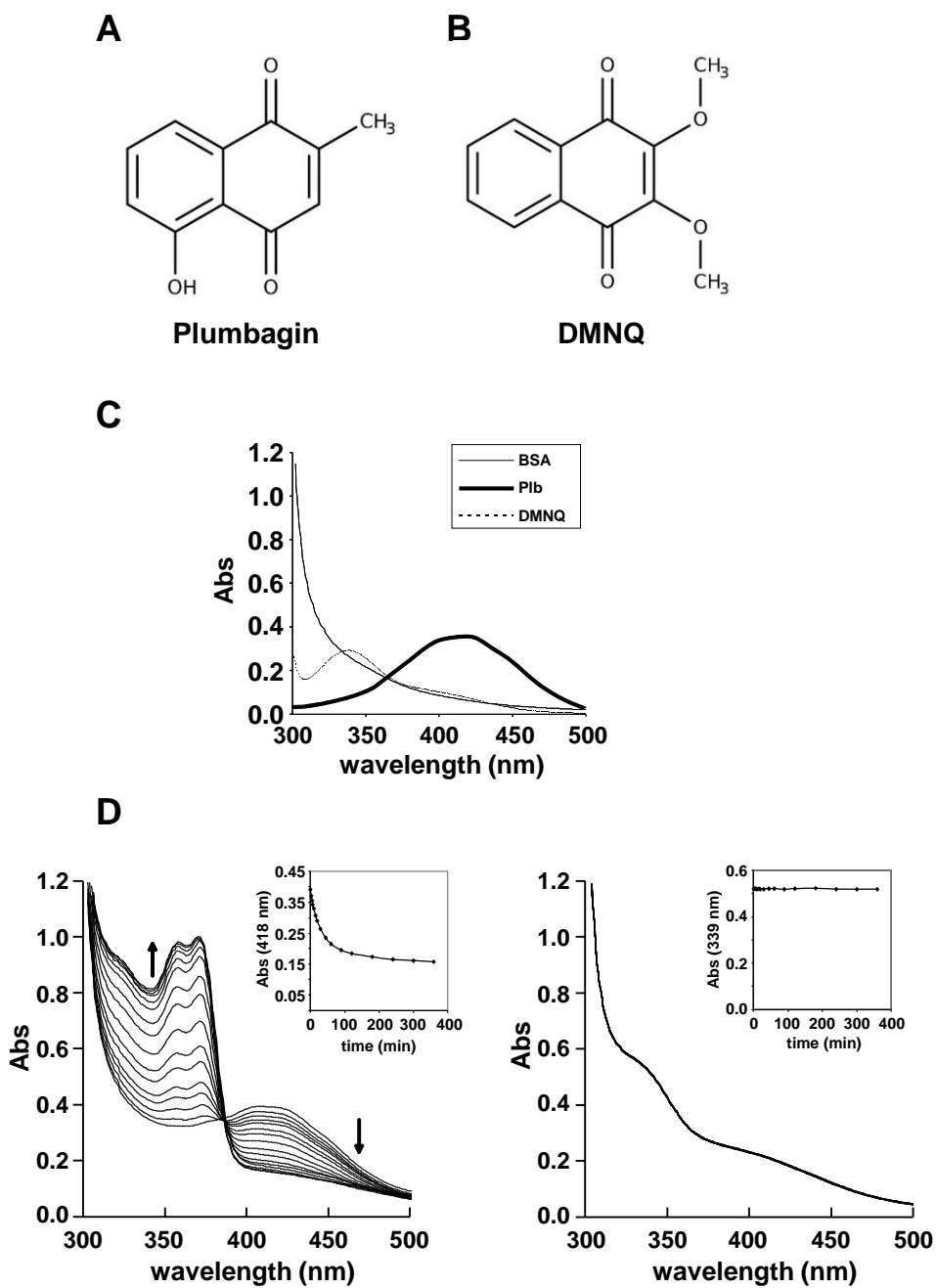
Figure 6: Western blot analysis of AR expression following plumbagin-albumin treatment.

Cells were incubated with plumbagin-BSA or with unconjugated BSA for the indicated times. Cells were lysed and relative protein amounts were analyzed by western blot. The membrane was stripped and probed several times with the indicated antibodies. **Panel A:** PTEN-P2 cells were treated with increasing concentrations of plumbagin-BSA for 24h. The insert shows the quantification of AR expression in this experiment. **Panel B:** PTEN-P2 cells were treated with 10 μ mol/L plumbagin-BSA for the indicated times. **Panel C:** Average AR expression following treatment with 10 μ mol/L of plumbagin conjugate for 24h. Values represent means \pm SE of 5 separate experiments. **Panel D:** Human cancer cells LNCaP were treated with plumbagin-HSA at 10 μ mol/L for 24h.

Figure 7: Western blot analysis of PKC expression and AMPK phosphorylation following plumbagin-albumin treatment.

Cells were incubated with plumbagin-BSA or with BSA for various times of treatment, lysed, and the relative protein expression was analyzed by western blot. The membrane was stripped and probed several times. **Panel A:** PTEN-P2 cells were treated with 10 μ mol/L plumbagin-BSA for up to 48h. PKC ϵ , PKC μ and PKC δ were sequentially analyzed by western blot using isoform-specific antibodies. **Panel B:** Average PKC ϵ expression following treatment with 10 μ M of plumbagin conjugate for 24h. Values represent means \pm SE of 5 separate experiments. **Panel C:** PTEN-P2 cells were treated with

10 μ M plumbagin-BSA for up to 4 hours. A pan phospho-PKC (β II-Ser660) antibody was used to measure PKC phosphorylation. Phospho-AMPK α (Thr172) and phospho-ACC (Ser79) were sequentially analyzed by western blot using phosphor-isoform-specific antibodies. **Panel D:** Average AMPK α phosphorylation following treatment with 10 μ mol/L of plumbagin conjugate for 30min and 1h (peak). Values represent means \pm SE of 5 separate measurements from 2 independent experiments.

**FIGURE 1**

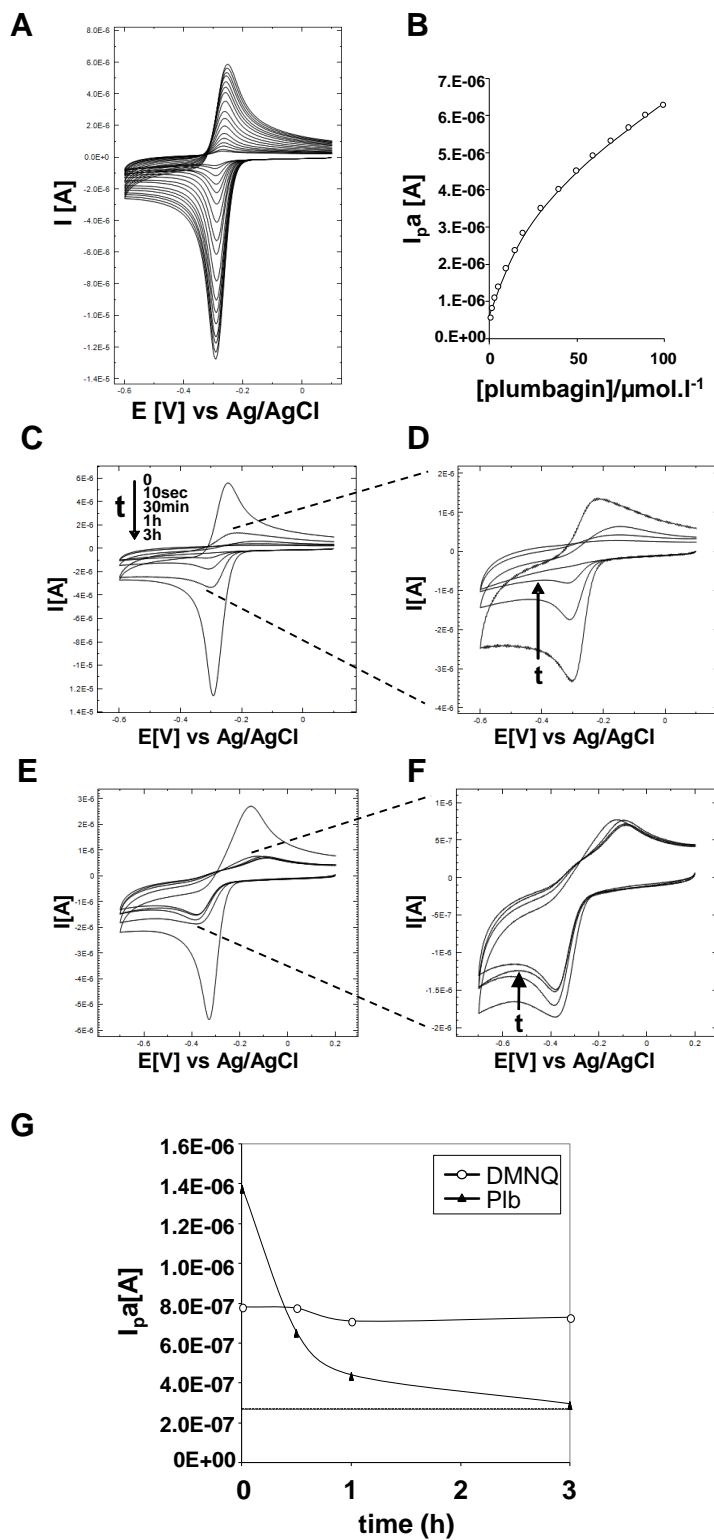


FIGURE 2

This article is protected by copyright. All rights reserved.

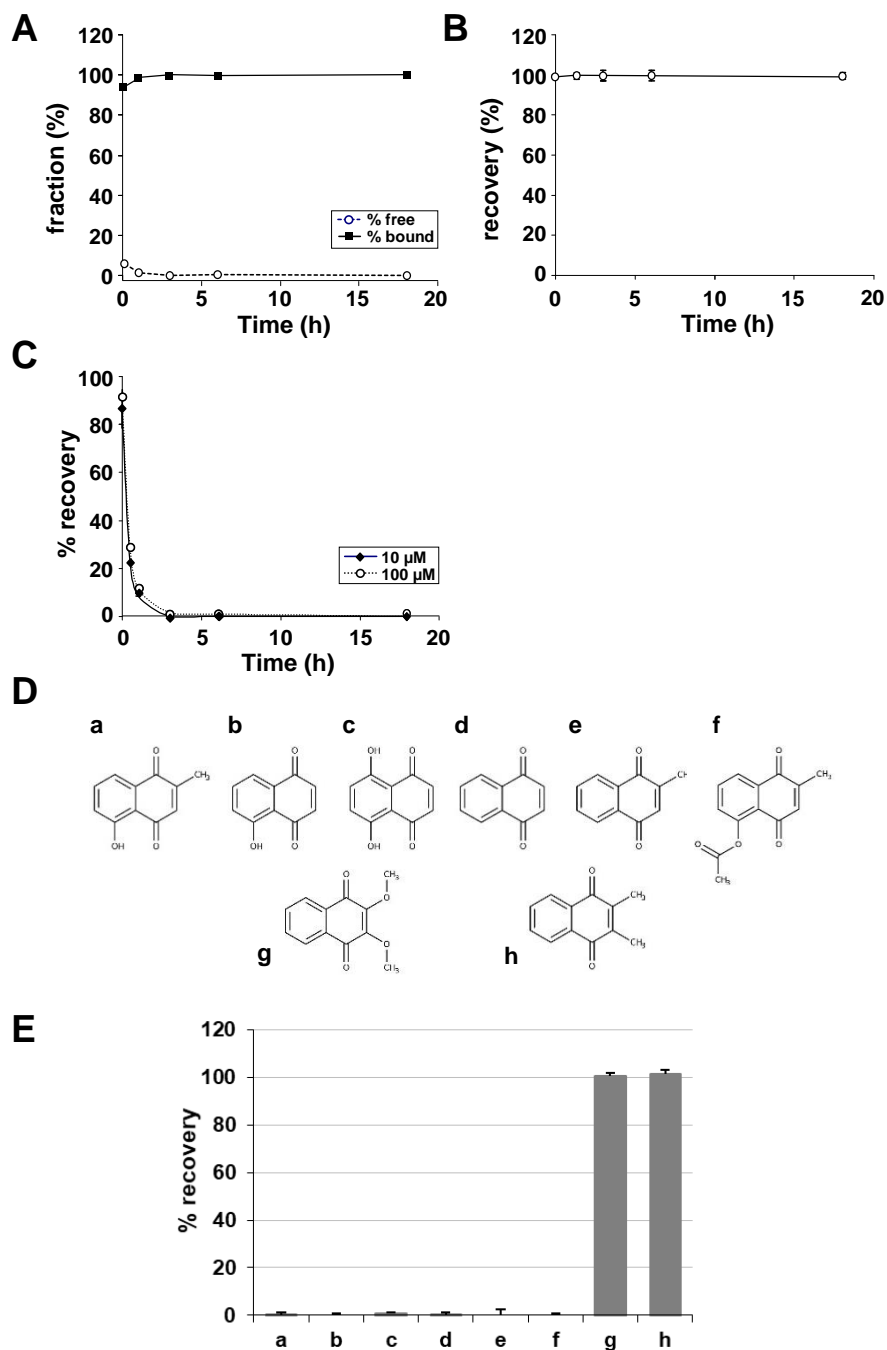
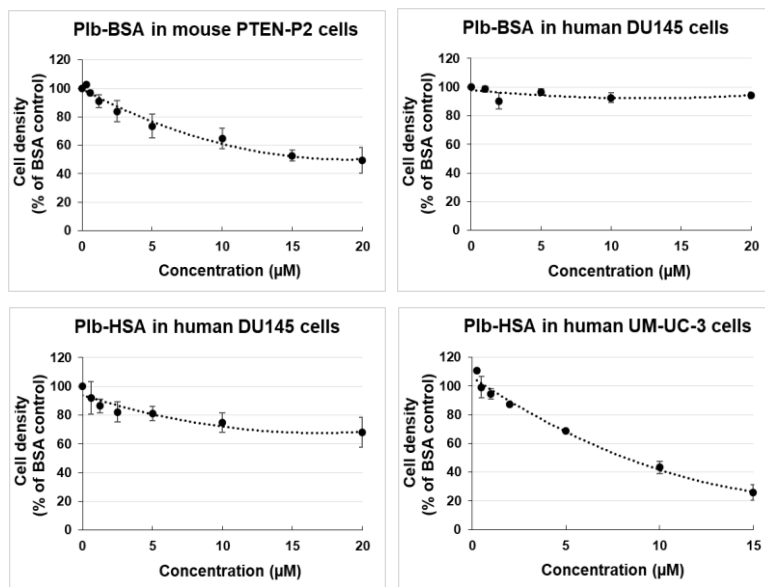
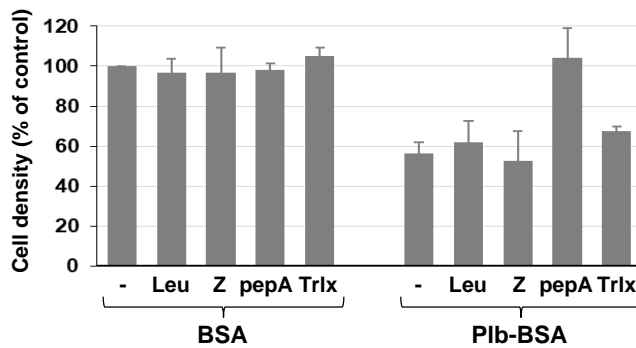
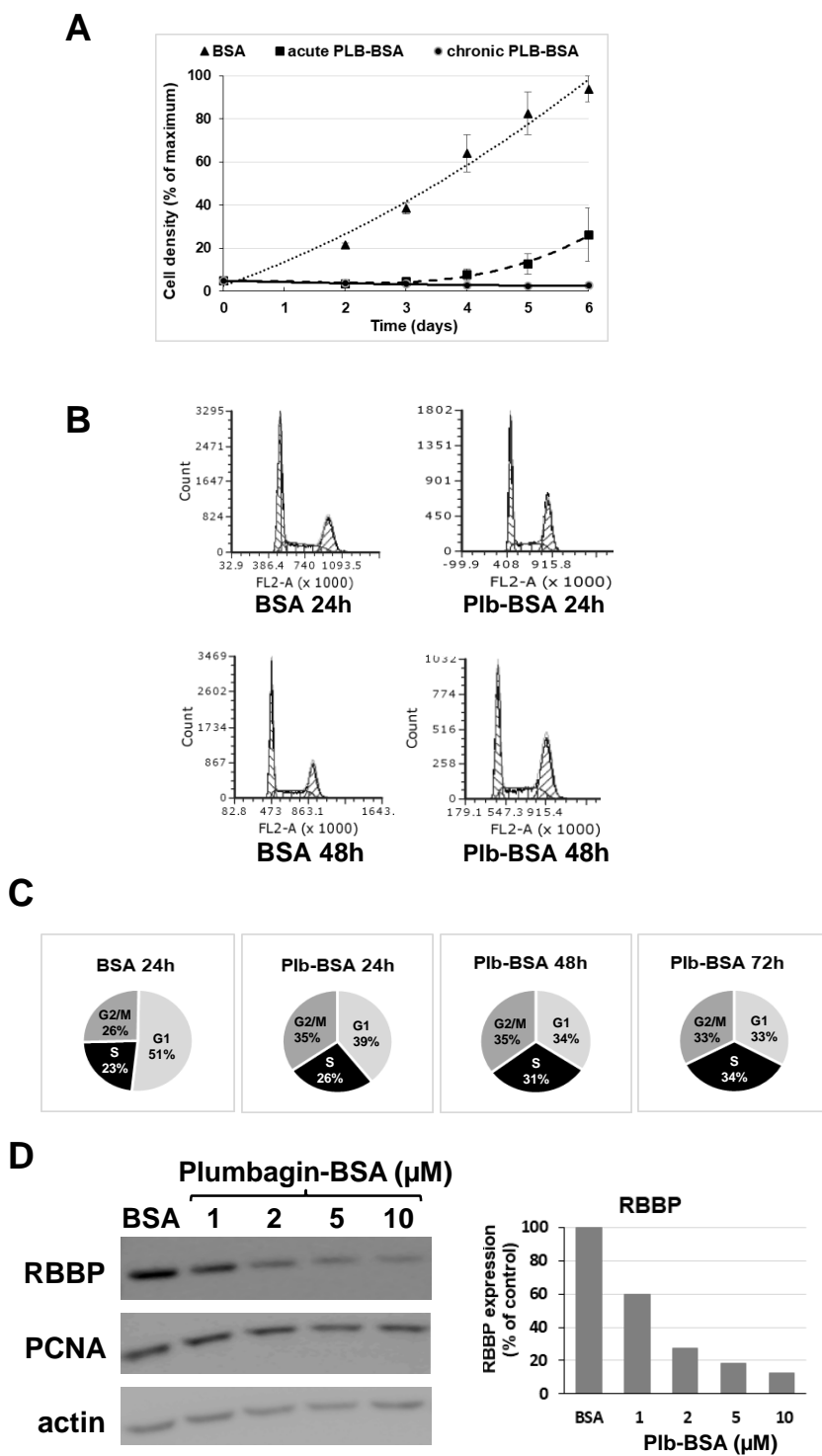


FIGURE 3

A**B****FIGURE 4**

**FIGURE 5**

This article is protected by copyright. All rights reserved.

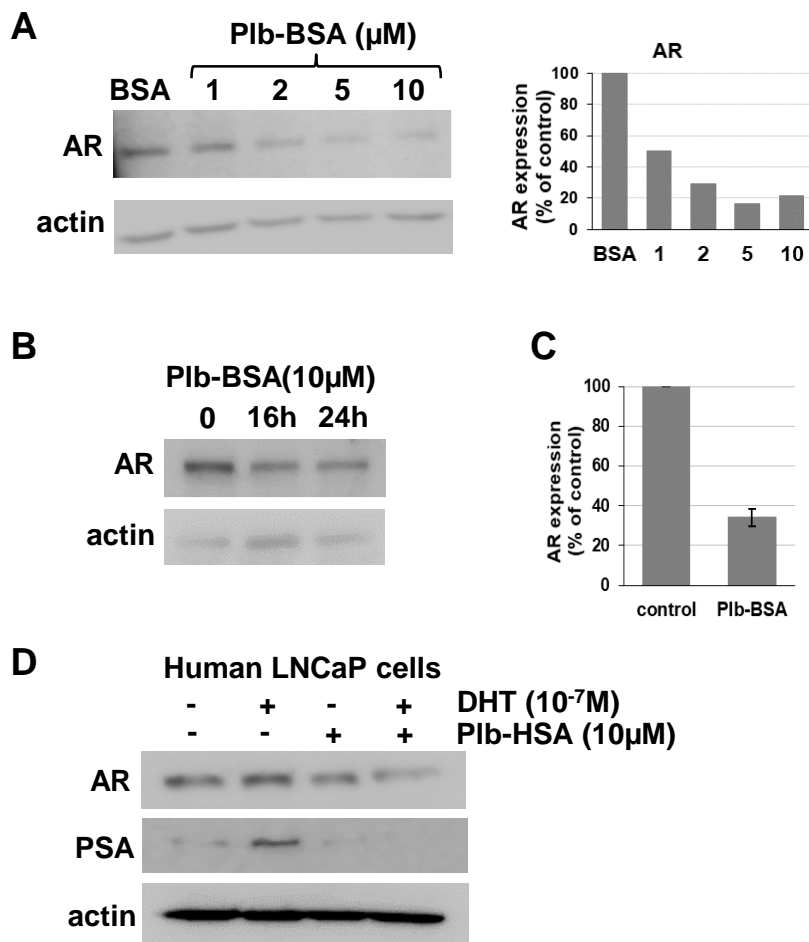
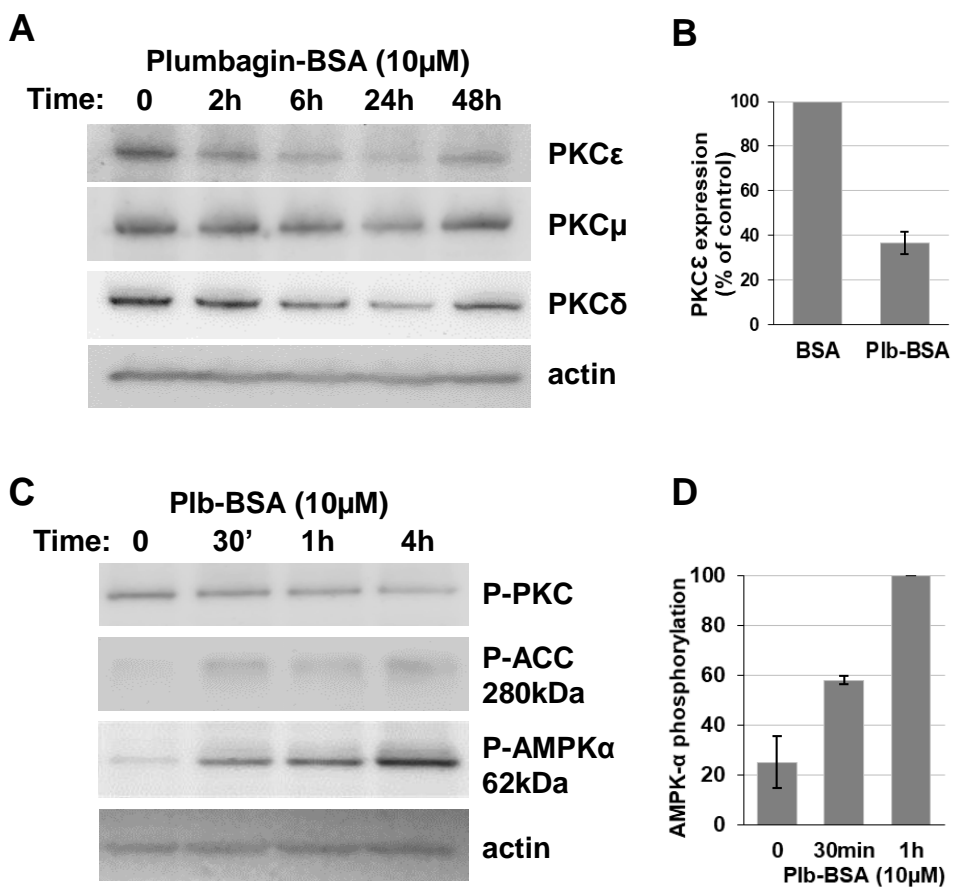


FIGURE 6

**FIGURE 7**